Cell Stem Cell

Article

Overcoming Intrinsic H3K27me3 Imprinting Barriers Improves Post-implantation Development after Somatic Cell Nuclear Transfer

Graphical Abstract

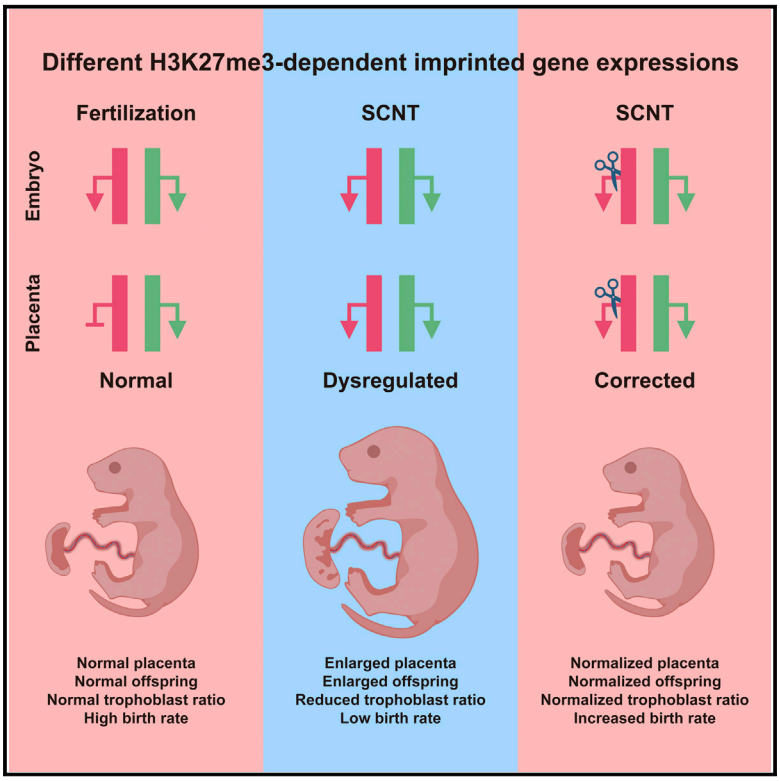

Highlights

- Increased SCNT cloning by monoallelic deletion of four H3K27me3-imprinted genes
- H3K27me3-imprinted gene deletion normalized body and placental weights in cloned pups
- Sfmbt2 deletion is the most effective monoallelic deletion for improving SCNT

Authors

Le-Yun Wang, Zhi-Kun Li, Li-Bin Wang, ..., Fa-Long Lu, Wei Li, Qi Zhou

Correspondence

fllu@genetics.ac.cn (F.-L.L.), liwei@ioz.ac.cn (W.L.), zhouqi@ioz.ac.cn (Q.Z.)

In Brief

Wang et al. report significantly increased cloning efficiencies from fibroblasts by engineering monoallelic deletions of four placenta-specific H3K27me3 imprinting genes. Editing in and deriving donor cells from haploid embryonic stem cells enabled derivation of cloned pups with normalized body and placental weights.

Wang et al., 2020, Cell Stem Cell *27*, 315–325
August 6, 2020
https://doi.org/10.1016/j.stem.2020.05.014

CellPress

Cell Stem Cell

CellPress

Article

Overcoming Intrinsic H3K27me3 Imprinting Barriers Improves Post-implantation Development after Somatic Cell Nuclear Transfer

Le-Yun Wang,[1,3,6] Zhi-Kun Li,[1,3,6] Li-Bin Wang,[1,3,6] Chao Liu,[1,2,3,6] Xue-Han Sun,[1,2,3,6] Gui-Hai Feng,[1,3,6] Jia-Qiang Wang,[1,4] Yu-Fei Li,[1,3] Lian-Yong Qiao,[5] Hu Nie,[2,5] Li-Yuan Jiang,[1,4] Hao Sun,[1,2,3] Ya-Li Xie,[2,5] Si-Nan Ma,[1,4] Hai-Feng Wan,[1,3] Fa-Long Lu,[5,*] Wei Li,[1,3,*] and Qi Zhou[1,3,7,*]

[1]State Key Laboratory of Stem Cell and Reproductive Biology, Institute of Zoology, Chinese Academy of Sciences, Beijing 100101, China
[2]University of the Chinese Academy of Sciences, Beijing 100049, China
[3]Institute for Stem Cell and Regeneration, Chinese Academy of Sciences, Beijing 100101, China
[4]College of Life Science, Northeast Agricultural University, Harbin 150030, China
[5]State Key Laboratory of Molecular Developmental Biology, Institute of Genetics and Developmental Biology, Chinese Academy of Sciences, Beijing 100101, China
[6]These authors contributed equally
[7]Lead Contact
*Correspondence: fllu@genetics.ac.cn (F.-L.L.), liwei@ioz.ac.cn (W.L.), zhouqi@ioz.ac.cn (Q.Z.)
https://doi.org/10.1016/j.stem.2020.05.014

SUMMARY

Successful cloning by somatic cell nuclear transfer (SCNT) requires overcoming significant epigenetic barriers. Genomic imprinting is not generally regarded as such a barrier, although H3K27me3-dependent imprinting is differentially distributed in E6.5 epiblast and extraembryonic tissues. Here we report significant enhancement of SCNT efficiency by deriving somatic donor cells carrying simultaneous monoallelic deletion of four H3K27me3-imprinted genes from haploid mouse embryonic stem cells. Quadruple monoallelic deletion of *Sfmbt2*, *Jade1*, *Gab1*, and *Smoc1* normalized H3K27me3-imprinted expression patterns and increased fibroblast cloning efficiency to 14% compared with a 0% birth rate from wild-type fibroblasts while preventing the placental and body overgrowth defects frequently observed in cloned animals. *Sfmbt2* deletion was the most effective of the four individual gene deletions in improving SCNT. These results show that lack of H3K27me3 imprinting in somatic cells is an epigenetic barrier that impedes post-implantation development of SCNT embryos and can be overcome by monoallelic imprinting gene deletions in donor cells.

INTRODUCTION

Somatic cell nuclear transfer (SCNT) can be used to reprogram a somatic nucleus to its totipotent state, and it has great potential for use in animal production and regenerative medicine (Rideout et al., 2001). However, the extremely low efficiency and frequently observed abnormalities in SCNT embryos indicate the existence of epigenetic barriers to somatic cell reprogramming (Lu and Zhang, 2015). Among these abnormalities, large offspring syndrome (LOS) is one of the most common and is seen in cloned cattle, sheep, and mice. This refers to a heterogeneous group of symptoms, including large size at birth and severe birth defects (Yang et al., 2007). Progress has been made in identifying and overcoming critical epigenetic barriers, including inhibiting histone deacetylation, reducing DNA methylation, and removing soma-persisting H3K9me3 (Dai et al., 2010; Gao et al., 2018; Kishigami et al., 2006; Matoba et al., 2014), all of which significantly improve the development of SCNT embryos but have little effect on defects found in all cloned mammals. Although aberrant imprinting is also observed in cloned animals, canonical genomic imprinting mediated by DNA methylation is relatively stable and falls beyond the current ability to perform ooplasm reprogramming (Humpherys et al., 2001; Inoue et al., 2002; Okae et al., 2014). For example, primordial germ cell cloning cannot restore a deficient imprinting status or produce viable pups (Inoue et al., 2002; Kamimura et al., 2014; Lee et al., 2002; Tucci et al., 2019). For these reasons, genomic imprinting is not usually regarded as an epigenetic barrier to SCNT (Fulka et al., 2004; Kamimura et al., 2014).

Large placentae are, like LOS, frequently observed during gestation of cloned animals, regardless of the donor cell type (Wakisaka-Saito et al., 2006). Overgrowth of the spongiotrophoblast is a typical feature of placental abnormalities in SCNT (Tanaka et al., 2001). Extraembryonic defects can also contribute to the low success rate of SCNT. Recently, 76 putative H3K27me3-dependent imprinting genes were identified in the mouse morula whose imprinting was largely lost with development of the embryo (Inoue et al., 2017a). The detailed physiological function of these noncanonical imprinting genes remains to be learned. Interestingly, imprinting of four genes

(*Sfmbt2*, *Smoc1*, *Jade1*, and *Gab1*) is specifically maintained in extraembryonic tissues until embryonic day 9.5 (E9.5), but it is lost in the epiblast by E6.5 (Inoue et al., 2017a). Because all somatic donor cells used for SCNT are epiblast descendants, it is natural to ask whether their expression patterns are intrinsically aberrant in SCNT-derived extraembryonic tissues.

RESULTS

Abnormal Biallelic Expression of H3K27me3 Imprinting Genes in the E19.5 SCNT Placenta

To investigate the allele-specific expression of H3K27me3 imprinting genes, we crossed two inbred mouse strains, C57BL/6-Tg(CAG-EGFP)1Osb/J (C57, mother) and PWK/PhJ (PWK, father) and performed SCNT with the cumulus cells of the adult F1 progenies of the crossed strains as donor cells. We also performed *in vitro* fertilization (IVF) with the oocytes and sperm of C57 (GFP+) and PWK to derive mouse embryo controls. Because the imprinting status of these genes has not been tested after E9.5 (Inoue et al., 2017a), we analyzed the SCNT and IVF embryos collected at E10.5. To avoid possible maternal cell contamination, placental cells derived from IVF and SCNT were purified with fluorescence-activated cell sorting (FACS) using the GFP signal and used for RNA sequencing (RNA-seq) analyses.

Three of the four H3K27me3 imprinting coding genes known to be specifically imprinted in the placenta (*Sfmbt2*, *Gab1*, and *Smoc1*) were overexpressed more than 2-fold in the SCNT placenta than in the IVF control (Figure 1A), but only *Sfmbt2* was overexpressed in the cloned fetus (Figure S1A). In addition, *Xist* was also overexpressed by more than 2-fold in the placenta but not in the fetus of the SCNT embryo (Figure 1B; Figure S1B). Many canonical imprinting genes, including *H19*, *Meg3*, and *Cdkn1c*, were also aberrantly expressed in E10.5 cloned embryos (Figure 1A; Figure S1A), similar to a previous report of E13.5 cloned embryos (Okae et al., 2014). Parental origin analysis using single-nucleotide polymorphisms (SNPs) revealed that the expression patterns of canonical and H3K27me3 imprinting genes were maintained in the SCNT embryo (Figure S1C; Table S1). In contrast, the allele-specific expression patterns of the four H3K27me3 imprinting genes were lost in the placenta of the SCNT embryo but the canonical imprinting genes were not (Figure 1C; Table S1). To understand the imprinting status of the four H3K27me3 imprinting genes in the late-stage placenta, we isolated GFP-positive cells from E19.5 placentae of IVF and SCNT embryos and performed reverse-transcriptase PCR and Sanger sequencing analyses. The paternally biased expression patterns of the four genes were maintained until E19.5 in the IVF placentae but were lost in the SCNT placentae (Figure 1D). Further, H3K27me3 imprinting genes have been reported to exhibit loss of imprint in SCNT blastocysts (Matoba et al., 2018). Thus, the aberrant biallelic expression of the noncanonical imprinting genes was maintained throughout post-implantation development of the cloned embryos.

Monoallelic Deletion of Four H3K27me3 Imprinting Genes Greatly Enhances the Success Rate of SCNT

Somatic cells with quadruple monoallelic deletion of the four H3K27me3 imprinting genes are needed to recover the loss of H3K27me3 imprinting in SCNT embryos (Matoba and Zhang, 2018). Currently, allele-specific gene deletion can be achieved by targeting DNA sites with SNPs on different alleles or with a suboptimal, distance-dependent gene editing strategy (Paquet et al., 2016), neither of which is practical for generating quadruple monoallelic deletions in somatic cells or embryonic stem cells. Because mice with heterozygous mutations at Sfmbt2 or Gab1 are paternally infertile, it is also not possible to generate mice with quadruple monoallelic deletions by mating ones with different heterozygous mutations (Itoh et al., 2000; Miri et al., 2013).

We developed a multistep approach, applying haploid embryonic stem cells (haESCs) with three paternal DMR (Differentially Methylated Region) knockouts (KOs) (H19-, IG-, and Rasgrf1-DMR [haESC^{3KO}]) as deletion platforms of H3K27me3-dependent imprinting genes. haESC^{3KO} could produce normal mice through MII (Metaphase II) oocyte injection, which had identical imprinting gene expression patterns as fertilization-derived mice (Leighton et al., 1995; Li et al., 2018; Lin et al., 2003). haESC^{3KO} were derived from a previous study (Li et al., 2018). It is worth mentioning that mice produced by oocyte injection of haESCs were able to produce viable offspring by natural mating with wild-type (WT) males (Li et al., 2016, 2018).

We derived haESC^{3KO} with quadruple frameshift mutations at *Sfmbt2*, *Jade1*, *Smoc1*, and *Gab1* using CRISPR-Cas9-mediated gene editing (Δ4-haESC^{3KO}) (Figures S1D–S1H). After MII oocyte injection of Δ4-haESC^{3KO}, the reconstructed embryos (Δ4-embryo^{3KO}) were transferred into the oviduct of pseudopregnant mice (Figure 1E). However, development of Δ4-embryo^{3KO} was restricted to E9.5 by defective placentae, indicating indispensability of monoallelically expressed H3K27me3 imprinting genes in development of extraembryonic tissues (Figure 1F; Table S2).

To derive somatic donors with monoallelic H3K27me3 imprinting gene mutations, we used tetraploid complementation, in which the tetraploid host blastocyst primarily forms extraembryonic lineages, not the embryo proper (Nagy et al., 1990). We isolated the inner cell masses (ICMs) of pre-implantation Δ4-embryo^{3KO} and injected them into WT tetraploid blastocysts before recipient transfer (Figure 2A). The reconstructed embryos were able to develop into full-term mice (Table S2). The Δ4-embryo^{3KO} rescued by tetraploid blastocysts further confirmed that the embryos were restricted by deficient extraembryonic tissues. More importantly, mouse embryonic fibroblasts (MEFs) were successfully derived from rescued E13.5 Δ4-embryo^{3KO} (Δ4-MEF^{3KO}) (Figure 2A).

Using Δ4-MEF^{3KO} as donor cells, we performed SCNT to regain the monoallelic expression patterns of the four noncanonical imprinting genes in SCNT embryos. We previously reported that a modified SCNT culture medium (D medium) significantly increased the cloning blastocyst rate (Dai et al., 2009). However, the blastocyst rate of Δ4-MEF^{3KO} cloned embryos (Δ4-NT-embryo^{3KO}) was not better than that of the cloned embryos from WT MEFs, regardless of the presence (85.6% ± 4.8%) or absence (23.1% ± 2.7%) of D medium (Table S3). These results indicate that H3K27me3 imprinting deletions have no obvious effects on preimplantation development of SCNT embryos.

By performing immunofluorescence quantification with blastocysts of IVF-derived, WT somatic cell cloned and Δ4-MEF^{3KO} cloned embryos, we found that the signals of GAB1, JADE1,

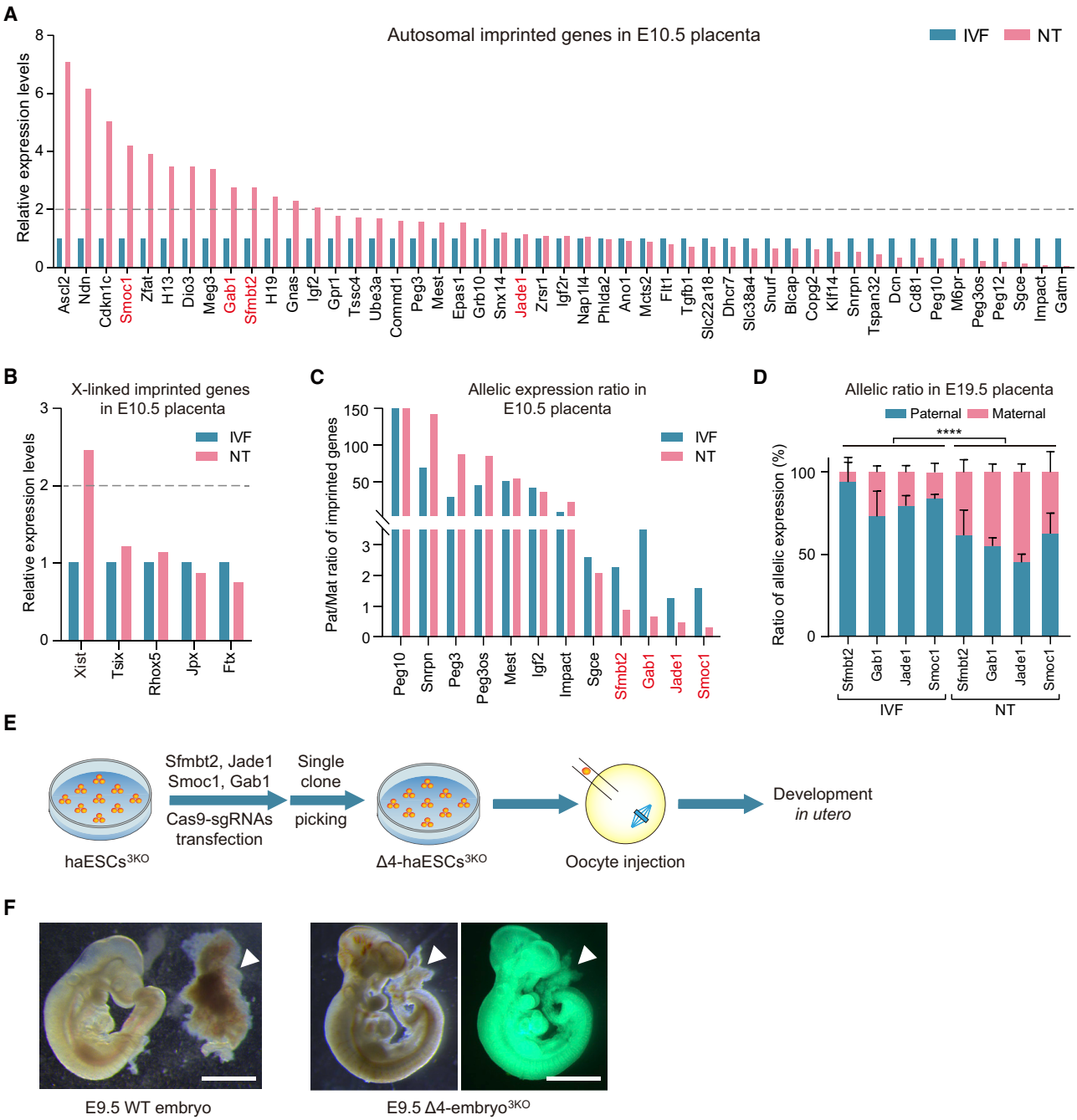

Figure 1. Loss of H3K27me3 Imprinting in Cloned Placentae

(A) Bar graphs showing relative gene expression levels of autosome imprinting genes in E10.5 SCNT placentae. Shown are 50 imprinting genes that can be reliably detected in SCNT placentae (FPKM > 1, n = 1). The expression level of the IVF placenta was set as 1. Gene names in red are H3K27me3 imprinting genes. The gray dashed line indicates overexpressed imprinting genes in SCNT placentae (FC > 2).

(B) Bar graphs showing relative gene expression levels of X-linked imprinting genes in E10.5 SCNT placentae (FPKM > 1, n = 1). The expression level of IVF placentae was set as 1. The gray dashed line indicates overexpressed imprinting genes in SCNT placentae (FC > 2).

(C) Bar graphs showing the ratio (paternal [Pat] divided by maternal [Mat]) of allelic expression of the canonical and H3K27me3-dependent imprinting genes in IVF and SCNT placentae identified by SNP (FPKM > 1, n = 1). Gene names in black and red are representative canonical and H3K27me3-dependent imprinting genes, respectively.

(D) The ratio of allelic expression of H3K27me3 imprinting genes was identified with SNPs from RT-PCR and Sanger sequencing of IVF and SCNT E19.5 placentae (n = 2). Data are presented as means ± SEM, ****$p < 0.0001$ according to two-way ANOVA.

(E) Scheme of four H3K27me3 imprinting gene deletions by haESC^{3KO} and MII oocyte injection.

(F) Left: WT E9.5 embryo and placenta. Right: restricted E9.5 Δ4-embryo^{3KO} and placenta. Placentae are indicated by white triangles. Scale bars, 0.5 mm.

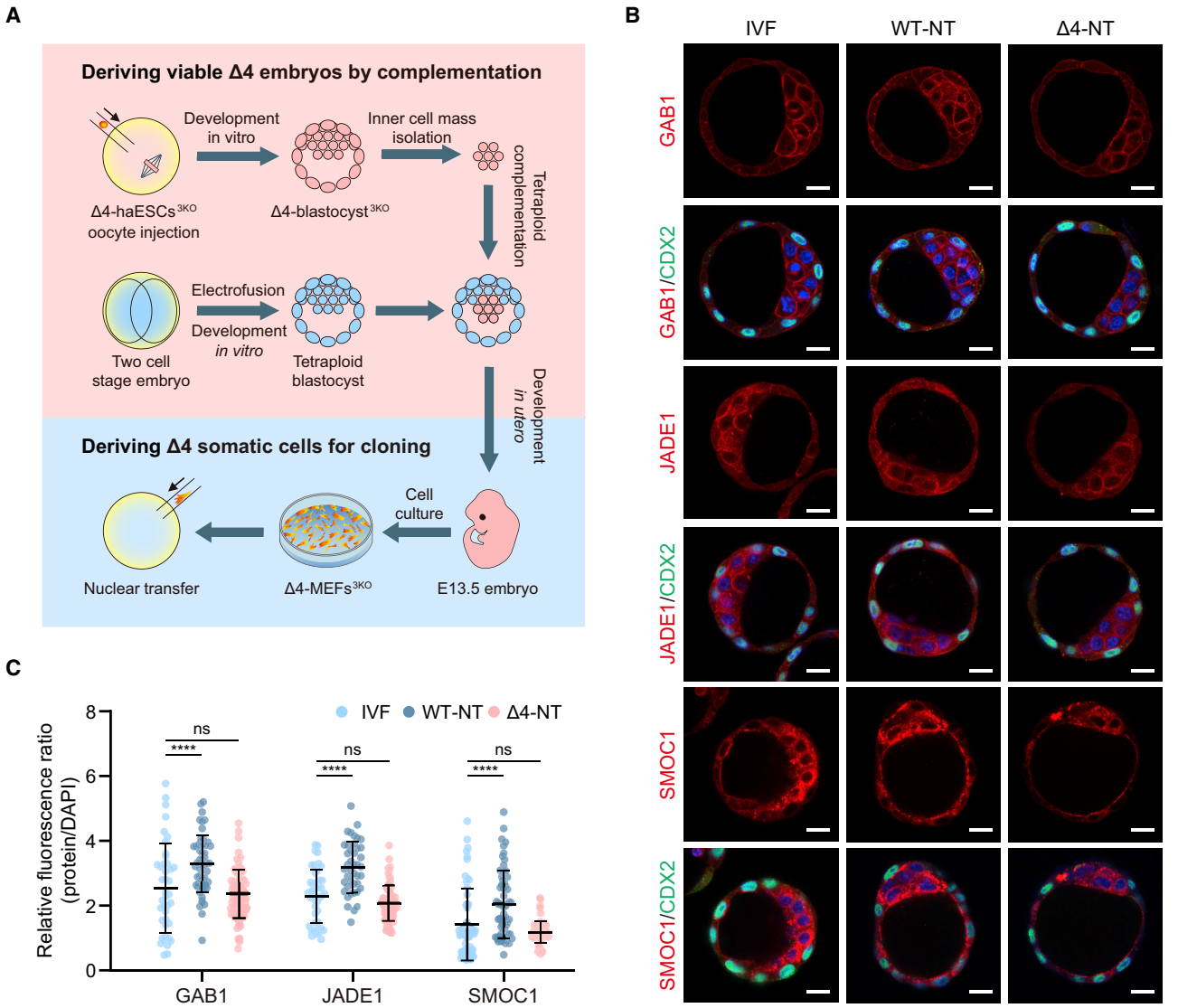

Figure 2. Deriving Somatic Cells with Quadruple Heterozygous Deletion of H3K27me3 Imprinting Genes for Cloning

(A) Scheme to derive E13.5 MEFs from complemented Δ4-embryo^{3KO} and cloning. The ICM of Δ4-embryo^{3KO} blastocysts was injected into WT tetraploid embryos before recipient transfer. Complemented Δ4-embryo^{3KO} were able to complete full-term development, as shown in Table S2. E13.5 MEFs were derived from the complemented Δ4-embryo^{3KO} and cloned to derive Δ4-NT-mouse^{3KO}. Red and blue shading represents derivation of viable Δ4 embryos by tetraploid complementation and derivation of E13.5 Δ4 MEFs for cloning, respectively.

(B) Immunofluorescence results of H3K27me3-dependent imprinting genes in IVF, WT-NT, and Δ4-NT blastocysts. Red signals indicate H3K27me3-dependent imprinting gene staining. Green signals indicate CDX2 staining. Blue signals indicate DNA DAPI staining. Scale bars, 15 μm.

(C) Immunofluorescence comparison of H3K27me3-dependent imprinting genes in TE cells of IVF-, WT-NT-, and Δ4-NT-derived blastocysts. Each dot represents the specific value of the protein/DAPI strength ratio of a single TE cell. Solid lines represent mean values and SD. ****$p < 0.0001$; ns, not significant; assessed by Student's t test.

and SMOC1 in the ICMs of IVF-derived embryos were comparable with those of the WT-NT derived embryos, but those in the trophectoderm (TE) cells (CDX2-positive) of IVF-derived embryos were weaker than those of WT-NT-derived (wild type-NT, i.e. NT without any treatment) embryos (Figure 2B). On the other hand, the ICM and TE signals of Δ4-MEF^{3KO} cloned embryos were weaker than those of WT-NT derived embryos, exhibiting effective downregulation of GAB1, JADE1, and SMOC1 protein levels after monoallelic deletions in somatic cell-cloned blastocysts (Figure 2B). Consistently, relative fluorescence ratio analyses revealed similar levels of H3K27me3 imprinting genes in TE cells of IVF-derived and Δ4-MEF^{3KO} cloned blastocysts that were lower than those of WT cell cloned blastocysts (Figure 2C), proving that overexpression of H3K27me3 imprinting genes in TE cells of somatic cell-cloned embryos was efficiently recovered by the deletions.

Next we transferred Δ4-NT-embryo^{3KO} into pseudopregnant recipient females at the two-cell stage. Remarkably, Δ4-NT-embryo^{3KO} exhibited a much higher implantation rate (68.4% ± 11.4%) than controls (6.1% ± 5.5%), comparable with that of IVF

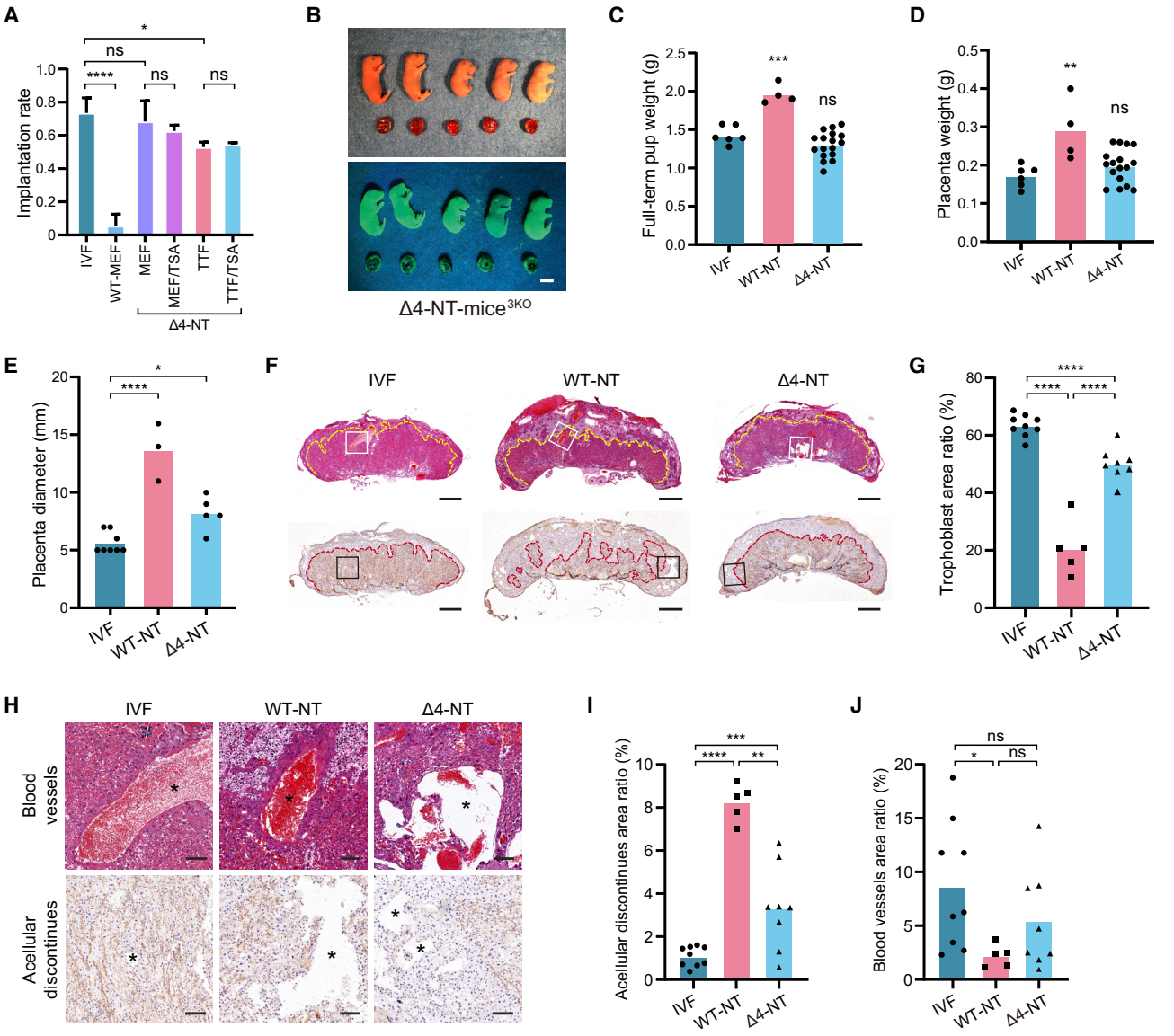

Figure 3. Development Results of Somatic Cell Cloned Embryos Carrying Quadruple Heterozygous Deletion of H3K27me3 Imprinting Genes

(A) A comparison of the implantation rates of IVF-, WT MEF-, and Δ4 MEF/Δ4 TTF-derived embryos with or without TSA treatment.

(B) Image of post-natal day 0 (P0) Δ4-NT-mouse^{3KO} and placentae in one experiment. Scale bar, 10 mm.

(C) Body weight comparison of full-term WT (n = 4) and Δ4-NT-mouse^{3KO} (n = 17). IVF pups (n = 6) were used as controls.

(D) Full-term placenta weight comparison in full-term WT (n = 4) and Δ4-NT-mouse^{3KO} (n = 17); IVF placentae (n = 6) were used as controls.

(E) Bar graph comparison of the placenta diameters of full-term WT and Δ4-NT-mouse^{3KO} placentae. IVF placentae were used as controls.

(F) Representative images of histological sections of E19.5 placentae stained with hematoxylin and eosin (top) and laminin α1 antibody (bottom). The yellow (top) and red (bottom) curves highlighted the fetal vasculature of the labyrinth. Scale bars, 1 mm.

(G) Bar graphs showing the area ratio of the fetal vasculature in the labyrinth.

(H) Blood vessels (top) and acellular discontinuities (Hackett et al., 2013) of full-term IVF, WT-NT, and Δ4-NT-mouse^{3KO} placentae. The presented regions are highlighted by the rectangles in (F). The regions marked with asterisks are acellular discontinuities and blood vessels, respectively. Scale bars, 0.15 mm.

(I) Bar graphs showing the area ratio of acellular discontinuities in the labyrinth.

(J) Bar graphs showing the area ratio of blood vessels in the labyrinth.

For all graphs, data are presented as means ± SEM. *p < 0.05, **p < 0.01, ***p < 0.001, ****p < 0.0001, assessed with Student's t test.

embryos (73.5% ± 7.8%) (Figure 3A). More encouragingly, after they completed full-term development, 8.5%–14.2% of transferred embryos were born as full-term pups (Δ4-NT-mouse^{3KO}), a significantly higher rate than in WT (0%) or cumulus cells (1.1% ± 0.2%) (Figure 3B; Table 1). The body weights of newborn Δ4-NT-mouse^{3KO} (1.28 ± 0.17 g) were similar to those of IVF mice (1.41 ± 0.11 g) and lower than those of WT cumulus cell cloned mice (1.94 ± 0.11 g) (Figure 3C). In addition, the placenta weights of Δ4-NT-mouse^{3KO} (0.19 ± 0.04 g) were comparable with those of IVF placentae (0.17 ± 0.03 g), which were significantly lower

Table 1. Development of SCNT Embryos from Enucleated Oocytes with Various Donor Cells

Groups	Donors	Cell Types	Sex of Somatic Cells	No. of Embryos Transferred	No. of Implantation Sites (% of Transferred Embryos)	No. of E8.5–E11.5 (% of Transferred Embryos)	No. of Full-Term Pups (% of Transferred Embryos)
Control	B6D2F1 MEFs	MEF	female	404	21 (5.2)	2 (0.5)	0 (0)^{A,B,C}
	B6D2F1 MEFs	MEF (TSA+)	female	161	23 (14.3)	4 (2.5)	0 (0)^{A,B,C}
	B6D2F1 TTFs	TTF	female	240	5 (2.1)	1 (0.4)	0 (0)^{D,E,F}
	B6D2F1 TTFs	TTF (TSA+)	female	94	15 (16.0)	2 (2.1)	0 (0)^{D,E,F}
	MEF^{3KO}	MEF	female	151	15 (9.9)	1 (0.7)	0 (0)^{A,B,C}
	TTF^{3KO}	TTF	female	171	3 (1.8)	0 (0)	0 (0)^{D,E,F}
	B6/PWK cumulus	cumulus	female	455	53 (11.6)	7 (1.5)	5 (1.1 ± 0.2)^{G}
	total	–	–	1,676	–	–	5
Δ4	Δ4-MEF^{3KO}-1	MEF	female	45	28 (62.2)	3 (6.7)	4 (8.6 ± 2.2)^{a,g,H,K,L}
	Δ4-MEF^{3KO}-1	MEF (TSA+)	female	68	43 (63.2)	6 (8.8)	6 (8.5 ± 2.6)^{h}
	Δ4-MEF^{3KO}-2	MEF	female	49	37 (75.5)	7 (14.3)	7 (14.2 ± 3.0)^{b,I}
	Δ4-TTF^{3KO}	TTF	female	64	34 (53.1)	6 (9.4)	3 (4.8 ± 1.0)^{d,I,J}
	Δ4-TTF^{3KO}	TTF (TSA+)	female	57	31 (54.4)	4 (7.0)	3 (5.3 ± 0.6)^{i}
	total	–	–	283	–	–	23
Δ4+ΔXist	ΔXist/Δ4 MEFs^{3KO}	MEF	female	78	40 (51.3)	7 (9.0)	4 (5.2 ± 0.8)^{c,k}
Single deletion	Smoc1$^{Δ/+}$ TTFs	TTF	female	137	5 (3.65)	0 (0)	0 (0)
	Gab1$^{Δ/+}$ TTFs	TTF	male	155	11 (7.1)	0 (0)	0 (0)
	Jade1$^{Δ/+}$ TTFs	TTF	female	52	24 (46.2)	4 (7.7)	0 (0)
	Sfmbt2$^{Δ/+}$ TTFs	TTF	female	112	50 (44.6)	5 (4.5)	3 (2.4 ± 2.3)^{e}
	Xist$^{Δ/Y}$ TTFs	TTF	male	134	65 (48.5)	7 (5.2)	0 (0)
Δ2	Δ2 TTFs	TTF	female	73	32 (43.8)	3 (4.1)	0 (0)
Δ3	Δ3 TTFs	TTF	female	88	47 (53.4)	8 (9.1)	4 (4.6 ± 0.6)^{f,j}
Total	–	–	–	2,788	–	–	39

For A versus a, B versus b, C versus c, D versus d, F versus f, and G versus g, $p < 0.01$. For E versus e, $p < 0.05$. For H versus h, I versus i, J versus j, K versus k, and L versus l, no significant difference. Δ2 represents monoallelic Sfmbt2 and Jade1 double deletion. Δ3 represents monoallelic Sfmbt2, Jade1, and Gab1 triple deletion. B6/PWK represents C57BL/6 × PWK/PhJ mice. "-1" and "-2" represent different E13.5 embryos to derive MEFs.

than those of WT cloned mice (0.29 ± 0.07 g) (Figure 3D). Consistent with this, the placenta diameters for Δ4-NT-mouse^{3KO} (8.2 ± 1.3 mm) were comparable with those of IVF placentae (5.6 ± 0.8 mm), which were significantly shorter than those of WT cloned mice (13.7 ± 2.0 mm) (Figure 3E). Western blot tests revealed decreased protein levels for H3K27me3 imprinting genes in the placentae of Δ4-NT-mouse^{3KO} (Figure S2A), which proved that the overexpression of H3K27me3 imprinting genes in cloned placentae was efficiently recovered by the deletions. In addition, RNA-seq analysis revealed similar brain transcriptomes in WT mice (n = 2) and Δ4-NT-mouse^{3KO} (n = 2), with an R^2 of 0.96 (Figure S2B). Hematoxylin and eosin staining and laminin α1 (a marker for fetal endothelium and its associated basement membrane) immunostaining showed that the fetal vasculature of the labyrinth was defective in cloned placentae from WT MEFs but significantly rescued in placentae of Δ4-NT-mouse^{3KO} (Figures 3F and 3G). In addition, acellular discontinuities in the feto-maternal interface and a low density of placental blood vessels were significantly rescued in Δ4-NT-mouse^{3KO} relative to WT cloned placentae (Figures 3H–3J; Georgiades et al., 2001).

To study the effects of H3K27me3 imprinting gene deletions in adult cell cloning, we obtained tail-tip fibroblasts (TTFs) from 6-week-old Δ4-NT-mouse^{3KO} (Δ4-TTFs^{3KO}) as donor cells for SCNT. Of the transferred Δ4-TTF^{3KO} cloned embryos, 4.8% ± 1.0% were born as full-term pups, which was significantly higher than the rate for WT TTFs (0%) (Table 1; Figure S2C). The cloning efficiency found in Δ4-MEF^{3KO} and Δ4-TTF^{3KO} was remarkable, considering the fact that, although mouse fibroblasts can be used to produce cloned offspring, they are among the least efficient donor cells (Ogura et al., 2013; Ono et al., 2001; Rideout et al., 2001; Wakayama and Yanagimachi, 1999, 2001). The viability of all Δ4-MEF/TTF cloned mice was traced. Of the 23 derived Δ4 cloned pups, 5 died before 21 days after birth, and 18 survived. This overall viability is not significantly different from that of WT cloned pups (1 of 5 died after birth) (Figure S2D). Taken together, these results demonstrate that correcting aberrant biallelic expression in the four H3K27me3 imprinting genes can significantly improve the pup rates of SCNT, even with adult-derived donor fibroblasts.

Impeding ectopic *Xist* expression may also considerably increase the rate of pup cloning (Inoue et al., 2010; Matoba et al., 2011). Therefore, we co-transfected Δ4-MEF^{3KO} with Cas9 and Xist-deleting sgRNA plasmids. Transfected Δ4-MEF^{3KO} were cloned and transferred into pseudopregnant

recipients. Viable E13.5 embryos were recovered using cesarean section, and Xist deletion was analyzed via PCR and Sanger sequencing. Embryos with monoallelic Xist deletion were chosen to derive MEFs (ΔXist/Δ4-MEF^{3KO}) for SCNT (Figure S3A). However, the pup rate for ΔXist/Δ4-MEF^{3KO} cloning (5.2% ± 0.8%) was not better than that of Δ4-MEF^{3KO}, indicating that Xist and four H3K27me3 imprinting gene deletions might not have had a synergic effect (Table 1; Figures S3B–S3D).

Recovering the *Xist* level does not improve pre-implantation development of SCNT embryos, as proven by the work of Matoba et al. (2011) showing that the blastocyst rate of Xist small interfering RNA (siRNA)-injected cloned embryos was not statistically different from that of embryos injected with control siRNA. It has also been proven that the implantation rates of somatic cells with monoallelic Xist deletion are not significantly better than those of WT cells when Sertoli or cumulus cells are used for cloning (Inoue et al., 2010). However, cumulus and Sertoli cells are highly efficient donors in SCNT, and both have high implantation rates in cloning relative to those of fibroblasts (Inoue et al., 2003; Ogura et al., 2000), limiting the space to assess improvements in implantation rate using Xist deletion. To better dissect the potential synergistic effects of Δ4 and ΔXist in cloning, we generated a maternal Xist-deleted mouse to derive Xist$^{\Delta/Y}$ TTFs as donor cells (Figure S3E). Consistent with these previous results, the blastocyst rate of Xist$^{\Delta/Y}$ TTF cloned embryos was not better than the cloned embryos from WT MEFs, regardless of the presence (83.2% ± 4.4%) or absence (25.1% ± 4.6%) of D medium (Table S3). Similar to the quadruple H3K27me3 imprinting gene deletions, the results showed that Xist deletion has no obvious effects on preimplantation development of SCNT embryos.

Next we transferred the Xist$^{\Delta/Y}$ TTF cloned embryos into pseudopregnant recipient females at the two-cell stage. To our surprise, 65 implantation sites were generated after 134 SCNT embryos were transferred, significantly higher than what was found for control TTFs (5 implantation sites of 240 transferred cloned embryos) (Table 1). This result proved that implantation rates of SCNT embryos could also benefit from monoallelic Xist deletion in somatic cells. Based on the overall survival rates of cloned embryos at five embryonic stages (two-cell stage/E1.0, implantation stage/E5.0, <E10.5, ≥E10.5, and full term), we found that Δ4 and ΔXist had very similar contributions in terms of cloning improvement patterns; both facilitated the implantation rates and post-implantation development of cloned embryos (Figures S3F and S3G). However, unlike the results of ΔXist/Δ4-MEF^{3KO} cloning, we did not derive any full-term pup from transfer of a limited number of 134 Xist-deleted SCNT embryos (Table 1). These results might provide an explanation for why Δ4 and ΔXist had no synergistic effect on SCNT development; the progress made by correcting the H3K27me3-dependent imprinting genes in cloned embryos somehow overlaps, whether from the autosomes or the X chromosome. On the other hand, our results also showed that Δ4 promoted full-term rates to a greater extent (six pups derived from 121 Δ4-TTF^{3KO} cloned embryos) than ΔXist when fibroblasts were used as donors for cloning (Table 1).

To study whether Δ4 has a synergistic effect with other methods of overcoming critical epigenetic barriers of SCNT, we treated Δ4-MEF^{3KO} cloned embryos with Trichostatin A (TSA), a histone deacetylase inhibitor known to improve cloning efficiency (Kishigami et al., 2006), and transferred them into pseudopregnant recipients. The pup rate of Δ4-MEF^{3KO} cloned embryos was not further increased, indicating that correcting the expression patterns of the four noncanonical imprinting genes and TSA treatment did not have a synergistic effect (Table 1).

To determine the fertility of Δ4-NT-mouse^{3KO}, we crossed them with WT males. Because all of the Δ4-NT-mouse^{3KO} were females, deletion of the four paternally expressed noncanonical imprinting genes did not compromise their expression or function in the offspring. As a result, Δ4-NT-mouse^{3KO} were able to give birth to viable offspring (Figure 4A). To calculate the litter size of Δ4-NT-mouse^{3KO}, the numbers of viable offspring (pups carrying no H19- or IG-DMR KOs) in each litter (n = 5) were multiplied by four, following the Mendelian ratio (Leighton et al., 1995; Li et al., 2018; Lin et al., 2003), and that rate was compared with that of WT females (n = 7). The corrected litter size of Δ4-NT-mouse^{3KO} was 6.80 ± 2.71, comparable with that of WT females (6.14 ± 1.80), indicating normal fertility in Δ4-NT-mouse^{3KO} (Figure 4B). In addition, RNA-seq analyses showed that Δ4-NT-mouse^{3KO} offspring had a normal transcriptome (Figure 4C).

Triple/Single Monoallelic Deletions of H3K27me3 Imprinting Genes in Fertilization-Derived Somatic Donor Cells Improves Placenta Development and the Pup Rate in SCNT

To further determine the contribution of each of the four H3K27me3 imprinting gene deletions, we derived TTFs from offspring with monoallelic deletion of single genes as donor cells for cloning (referred to as Sfmbt2$^{\Delta/+}$ TTFs, Jade1$^{\Delta/+}$ TTFs, Gab1$^{\Delta/+}$ TTFs, and Smoc1$^{\Delta/+}$ TTFs) (Figure S4A). Offspring devoid of H19, IG, or Rasgrf1 deletion were chosen for cloning (Figure S4B). Sfmbt2$^{\Delta/+}$ TTFs and Jade1$^{\Delta/+}$ TTFs had much greater implantation rates than WT TTFs after cloning (Table 1; Figure 4D). Although minor implantation rate increases were observed in the Gab1$^{\Delta/+}$ and Smoc1$^{\Delta/+}$ TTF cloned groups (Figure 4D), the differences are more likely to be due to the different genetic background in the WT and Gab1$^{\Delta/+}$/Smoc1$^{\Delta/+}$ mouse-derived TTFs than the effect of H3K27me3-dependent imprinting gene deletions. Notably, Sfmbt2$^{\Delta/+}$ TTF donors were able to produce full-term pups (Sfmbt2$^{\Delta/+}$-NT mice) with an efficiency of 2.4% ± 2.3%, significantly higher than that of WT TTFs (0%) (Figure 4E; Table 1). Because Sfmbt2$^{\Delta/+}$ TTF and Jade1$^{\Delta/+}$ TTF cloned embryos showed the most prominent effects on post-implantation development (Figure 4D), we also cloned TTFs with double monoallelic deletions (Sfmbt2$^{\Delta/+}$ and Jade1$^{\Delta/+}$ [Δ2 TTFs]) (Figure S4B). No full-term pup was derived from 73 transferred embryos, but the implantation rate of Δ2 TTFs (43.8%) was similar to that of Sfmbt2$^{\Delta/+}$ TTFs (44.6%) and Jade1$^{\Delta/+}$ TTFs (46.2%) (Table 1). Next we tested the SCNT efficiency of TTFs derived from offspring carrying monoallelic deletions of three genes (Sfmbt2$^{\Delta/+}$, Jade1$^{\Delta/+}$, and Gab1$^{\Delta/+}$ [Δ3 TTFs]). The implantation rate of Δ3 TTF cloned embryos (53.4%) was significantly higher than that of WT cloned embryos (Figure 4D; Table 1). In addition, Δ3 TTF cloned embryos produced full-term pups (Δ3-NT mice) with an efficiency of 4.6% ± 0.6%, comparable with that of Δ4-TTF^{3KO} (4.8% ± 1.0%) (Table 1; Figure S4C). The body weights of newborn Sfmbt2$^{\Delta/+}$-NT mice (1.26 ± 0.06 g)

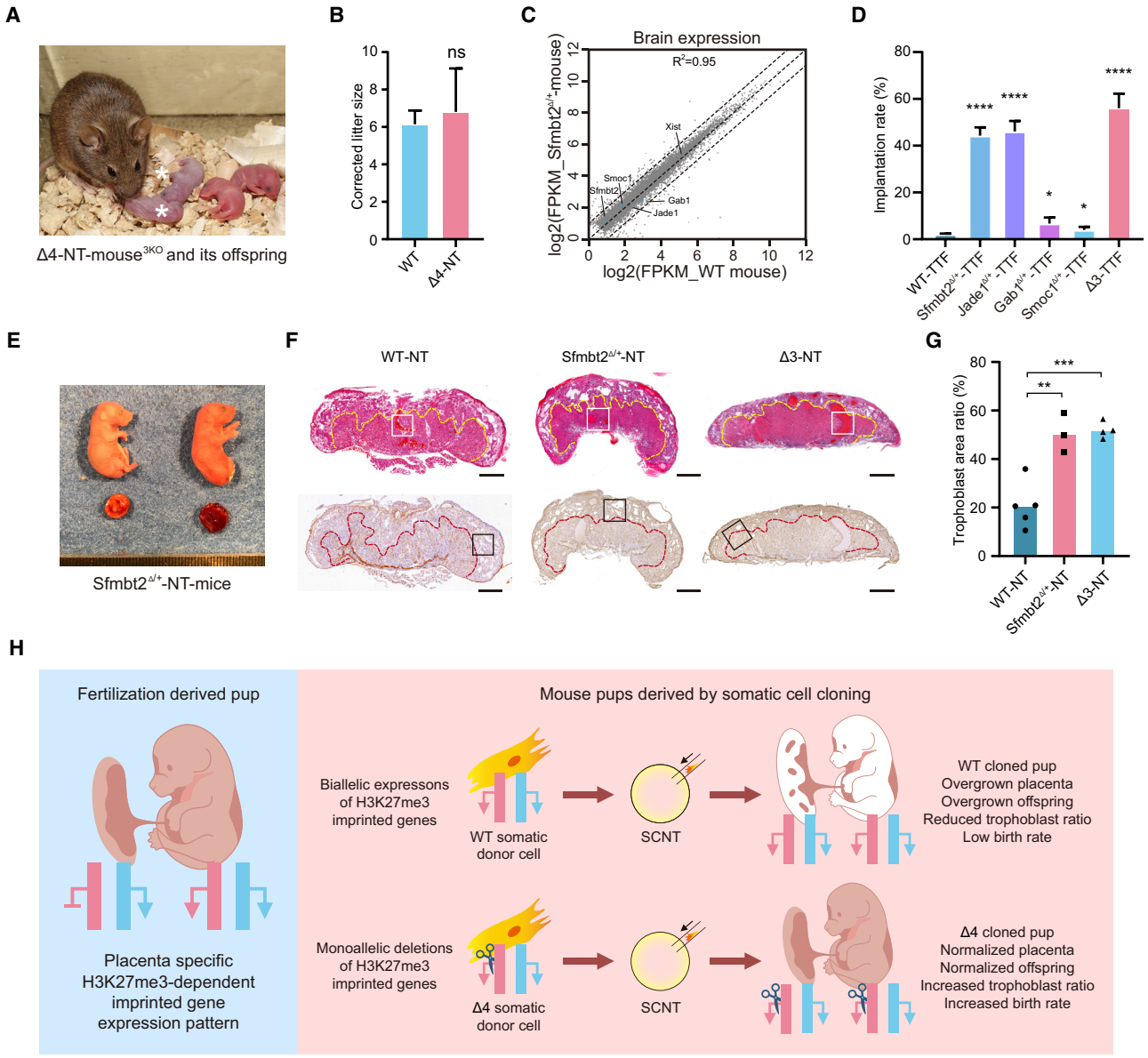

Figure 4. Correcting Individual H3K27me3 Imprinting Gene Improves SCNT Embryo Development to Varying Extents

(A) Image of Δ4-NT-mouse^{3KO} and their offspring. Offspring marked with an asterisk are dead pups that inherited KO IG-DMR from the mother.

(B) Corrected litter size of Δ4-NT-mouse^{3KO} was comparable with the WT.

(C) Brain transcriptome comparison of Δ4-NT-mouse^{3KO} offspring, Sfmbt2$^{Δ/+}$ mice, and WT mice; n = 2. R^2 was determined using Pearson's correlation.

(D) Comparison of the implantation rate for WT TTFs and Sfmbt2$^{Δ/+}$ TTFs, Jade1$^{Δ/+}$ TTFs, Gab1$^{Δ/+}$ TTFs, Smoc1$^{Δ/+}$ TTFs, and Δ3 TTFs.

(E) Image of Sfmbt2$^{Δ/+}$-NT mice.

(F) Representative images of histological sections of E19.5 placentae stained with hematoxylin and eosin (top) and laminin α1 antibody (bottom). The yellow (top) and red (bottom) curves highlight the fetal vasculature of the labyrinth. Scale bars, 1 mm.

(G) Bar graphs showing the area ratio of the fetal vasculature in the labyrinth.

(H) Scheme showing the placenta-specific imprinted pattern of H3K27me3 imprinting genes in fertilization-derived embryos, loss of imprint in the placentae of somatic cell cloned embryos, and rescue of low pup rate and placenta/offspring defects in SCNT embryos with heterozygous deletion of H3K27me3 imprinting genes.

For all graphs, data are presented as means ± SEM. *p < 0.05, **p < 0.01, ***p < 0.001, ****p < 0.0001, assessed with Student's t test.

and Δ3-NT mice (1.27 ± 0.08 g) were significantly lower than those of WT cloned mice (1.94 ± 0.11 g) (Figure S4D). The placenta weights of Δ3-NT mice (0.15 ± 0.02 g) were also significantly lower than those of WT cloned mice (0.29 ± 0.07 g) (Figure S4E). Placenta analysis indicated that the fetal vasculature of the labyrinth was significantly rescued in Sfmbt2$^{Δ/+}$-NT mice and Δ3-NT mice (Figures 4F and 4G), whereas the low density of blood vessels and acellular discontinuity were rescued in Δ3-NT mice but not in Sfmbt2$^{Δ/+}$-NT mice (Figures S4F–S4H; Georgiades et al., 2001).

DISCUSSION

LOS and large placentae have been observed in somatic cell cloned mice (Tamashiro et al., 2002), sheep (Fletcher et al., 2007), and cattle (Smith et al., 2012). It has been reported that placental overgrowth precedes fetal overgrowth, which has led to the hypothesis that fetal overgrowth could be an outcome rather than the cause of large placentae (Constant et al., 2006). In this study, we demonstrated that the development of SCNT placentae is significantly impeded by biallelically expressed H3K27me3 imprinting genes. Because H3K27me3 imprinting is intrinsically lost in epiblast-derived somatic lineages, H3K27me3 imprinting barriers might affect all cloned placentae when somatic cells are used as donors (Figure 4H).

After monoallelic deletion of H3K27me3 imprinting genes in somatic donor cells, the placenta weight, proportion of the fetus-derived vasculature labyrinth layer, blood vessel density, and acellular discontinuity in the placenta were well rescued. Further, the body weights of cloned mice were significantly recovered relative to WT cloned pups. Because loss of imprinting specifically takes place in the placenta, this recovery not only proves that aberrant placental H3K27me3 imprinting is responsible for LOS but also supports the hypothesis that dysregulated genes in the placenta might cause the LOS phenotype in cloned animals.

The H3K27me3 imprinting aberrance of SCNT blastocysts was first discovered by Matoba et al. (2018). However, the developmental significance of that discovery was not determined until this study. Unlike canonical imprinting genes, which are more randomly dysregulated in SCNT, noncanonical imprinting genes intrinsically feature loss of imprint (Figure 1C; Figure S1C). The distinction between canonical and noncanonical imprinting genes makes H3K27me3 a new category of dysregulated imprinting that affects all somatic cell cloned embryos and can explain the increase in pup rate following deletion of H3K27me3 imprinting genes.

Because genomic imprinting is completely erased and reestablished during germ cell development of the cloned animal (Fulka et al., 2004), the results of the offspring of TTF cloning proved that cloning of fertilization-derived (rather than haESC-derived) primary somatic cells could be supported by H3K27me3 imprinting gene deletions. More importantly, because offspring TTFs devoid of H19, IG, or Rasgrf1 deletion were used for cloning, the observed effect is solely due to the H3K27me3-imprinting deletions. We found that single monoallelic deletion ($Sfmbt2^{\Delta/+}$) was very effective for eliminating placental defects and increasing the pup rates of SCNT (although to a lesser degree than quadruple monoallelic deletions). Combined with the distance-dependent monoallelic editing technique of single genes in primary cells (Paquet et al., 2016), the method of H3K27me3 imprinting deletion might also be useful for wider applications.

It has been reported that H3K27me3 imprinting is also found in extraembryonic *Xist* silencing and lost in epiblast-derived lineages (Inoue et al., 2017b; Okamoto et al., 2011). As was the case in the four deleted H3K27me3 imprinting genes, we identified 2-fold overexpression of *Xist* in the SCNT placenta (Figure 1B). Notably, monoallelic deletion of *Xist* in Sertoli cells considerably increased the cloning pup rate from 1.6% to 15.4% (Inoue et al., 2010). These results indicate that loss of imprinting in *Xist* is another H3K27me3-dependent epigenetic barrier for SCNT. Recently, possible autosomal noncanonical imprinting genes have been identified in human embryos, suggesting that H3K27me3-dependent imprinting could be conserved in evolutionarily distant mammals (Zhang et al., 2019). However, the controversial result that H3K27me3 is globally depleted at the four- to eight-cell stage of human embryos as well as at the human XIST locus has been reported recently and indicates the absence of H3K27me3 imprinting events in humans (Xia et al., 2019). In addition, maternally specific *Xist* imprinting is not conserved in many species (Okamoto et al., 2011; Sado and Sakaguchi, 2013; Zou et al., 2019), which might limit the application of Xist deletion to improve animal cloning efficiency.

Fetus- or adult-derived fibroblasts are widely used in important large animal cloning, including, but not limited to, sheep (Schnieke et al., 1997), cattle (Cibelli et al., 1998), pigs (Onishi et al., 2000), and monkeys (Liu et al., 2018). However, in comparison with other donor cell types, mouse fibroblast cloning has been less efficient for a long time (Ogura et al., 2013; Wakayama and Yanagimachi, 1999, 2001). The results of our study show that the cloning efficiency of fetus- and adult-derived fibroblasts was increased significantly after H3K27me3-dependent imprinting gene deletion. More importantly, Δ4 or Sfmbt2 deletion promoted full-term rates at a greater extent than ΔXist when fibroblasts were used as donors. We not only demonstrated loss of H3K27me3-dependent imprinting as an intrinsic post-implantation epigenetic barrier in SCNT-mediated cloning, contributing to large placenta and offspring defects, but also confirmed that correcting H3K27me3 imprinting could be an avenue to increase the efficiency of animal cloning.

STAR★METHODS

Detailed methods are provided in the online version of this paper and include the following:

- KEY RESOURCES TABLE
- RESOURCE AVAILABILITY
  - Lead Contact
  - Materials Availability
  - Data and Code Availability
- EXPERIMENTAL MODEL AND SUBJECT DETAILS
  - Animal care and use
- METHOD DETAILS
  - Oocyte collection
  - CRISPR-Cas9 mediated gene deletions
  - Intracytoplasmic injection of $\Delta4\text{-haESCs}^{3KO}$
  - Blastocyst analysis by immunostaining
  - Tetraploid embryo complementation of ICM cells
  - Preparation of somatic donor cells for nuclear transfer
  - Somatic cell nuclear transfer and embryo culture
  - Embryo transfer
  - Immunohistochemistry staining and histological analysis
  - Placental RNA extraction and reverse transcription PCR
  - RNA-Seq library preparation and data analysis

- Western blot
- Southern blot

- QUANTIFICATION AND STATISTICAL ANALYSIS

SUPPLEMENTAL INFORMATION

Supplemental Information can be found online at https://doi.org/10.1016/j.stem.2020.05.014.

ACKNOWLEDGMENTS

We thank Cheng-He Li and Wen-Qiang Gan from the Institute of Materia Medica, Chinese Academy of Medical Sciences, and Peking Union Medical College for help with pathological sections. We thank Ming Ge, Wei-Yu Jin, Pei-Pei Long, and Zhi Liu from the Institute of Zoology, Chinese Academy of Sciences for technical assistance. This work was supported by the Strategic Priority Research Program of the Chinese Academy of Sciences (XDA16030403 to W.L.), the National Key Research and Development Program (2017YFA0103803 to Q.Z., 2018YFA0107703 to W.L., and 2018YFA0107001 to F.L.L.), the National Natural Science Foundation of China (31621004 to Q.Z. and W.L., 31701286 to G.F., and 31972895 to L.W.), the Key Research Projects of the Frontier Sciences of the Chinese Academy of Sciences (QYZDY-SSW-SMC002 to Q.Z. and QYZDB-SSW-SMC022 to W.L.), and the National Postdoctoral Program for Innovative Talents (BX201600161 and BX201700243).

AUTHOR CONTRIBUTIONS

L.-Y.W., Z.-K.L., F.-L.L., W.L., and Q.Z. conceived and designed the study. L.-Y.W., Z.-K.L., L.-B.W., C.L., X.-H.S., G.-H.F., J.-Q.W., Y.-F.L., L.-Y.Q., H.N., L.-Y.J., H.S., Y.-L.X., S.-N.M., and H.-F.W. performed the experiments. L.-Y.W. and Z.-K.L. analyzed the data. F.-L.L., W.L., and Q.Z. supervised the project. L.-Y.W., Z.-K.L., F.-L.L., W.L., and Q.Z. designed and wrote the manuscript.

DECLARATION OF INTERESTS

The authors declare no competing interests.

Received: September 27, 2019
Revised: January 13, 2020
Accepted: May 27, 2020
Published: June 18, 2020

REFERENCES

Cibelli, J.B., Stice, S.L., Golueke, P.J., Kane, J.J., Jerry, J., Blackwell, C., Ponce de León, F.A., and Robl, J.M. (1998). Cloned transgenic calves produced from nonquiescent fetal fibroblasts. Science *280*, 1256–1258.

Constant, F., Guillomot, M., Heyman, Y., Vignon, X., Laigre, P., Servely, J.L., Renard, J.P., and Chavatte-Palmer, P. (2006). Large offspring or large placenta syndrome? Morphometric analysis of late gestation bovine placentomes from somatic nuclear transfer pregnancies complicated by hydrallantois. Biol. Reprod. *75*, 122–130.

Dai, X., Hao, J., and Zhou, Q. (2009). A modified culture method significantly improves the development of mouse somatic cell nuclear transfer embryos. Reproduction *138*, 301–308.

Dai, X., Hao, J., Hou, X.J., Hai, T., Fan, Y., Yu, Y., Jouneau, A., Wang, L., and Zhou, Q. (2010). Somatic nucleus reprogramming is significantly improved by m-carboxycinnamic acid bishydroxamide, a histone deacetylase inhibitor. J. Biol. Chem. *285*, 31002–31010.

Fletcher, C.J., Roberts, C.T., Hartwich, K.M., Walker, S.K., and McMillen, I.C. (2007). Somatic cell nuclear transfer in the sheep induces placental defects that likely precede fetal demise. Reproduction *133*, 243–255.

Fulka, J., Jr., Miyashita, N., Nagai, T., and Ogura, A. (2004). Do cloned mammals skip a reprogramming step? Nat. Biotechnol. *22*, 25–26.

Gao, R., Wang, C., Gao, Y., Xiu, W., Chen, J., Kou, X., Zhao, Y., Liao, Y., Bai, D., Qiao, Z., et al. (2018). Inhibition of Aberrant DNA Re-methylation Improves Post-implantation Development of Somatic Cell Nuclear Transfer Embryos. Cell Stem Cell *23*, 426–435.e5.

Georgiades, P., Watkins, M., Burton, G.J., and Ferguson-Smith, A.C. (2001). Roles for genomic imprinting and the zygotic genome in placental development. Proc. Natl. Acad. Sci. USA *98*, 4522–4527.

Hackett, J.A., Sengupta, R., Zylicz, J.J., Murakami, K., Lee, C., Down, T.A., and Surani, M.A. (2013). Germline DNA demethylation dynamics and imprint erasure through 5-hydroxymethylcytosine. Science *339*, 448–452.

Humpherys, D., Eggan, K., Akutsu, H., Hochedlinger, K., Rideout, W.M., 3rd, Biniszkiewicz, D., Yanagimachi, R., and Jaenisch, R. (2001). Epigenetic instability in ES cells and cloned mice. Science *293*, 95–97.

Inoue, K., Kohda, T., Lee, J., Ogonuki, N., Mochida, K., Noguchi, Y., Tanemura, K., Kaneko-Ishino, T., Ishino, F., and Ogura, A. (2002). Faithful expression of imprinted genes in cloned mice. Science *295*, 297.

Inoue, K., Ogonuki, N., Mochida, K., Yamamoto, Y., Takano, K., Kohda, T., Ishino, F., and Ogura, A. (2003). Effects of donor cell type and genotype on the efficiency of mouse somatic cell cloning. Biol. Reprod. *69*, 1394–1400.

Inoue, K., Kohda, T., Sugimoto, M., Sado, T., Ogonuki, N., Matoba, S., Shiura, H., Ikeda, R., Mochida, K., Fujii, T., et al. (2010). Impeding Xist expression from the active X chromosome improves mouse somatic cell nuclear transfer. Science *330*, 496–499.

Inoue, A., Jiang, L., Lu, F., Suzuki, T., and Zhang, Y. (2017a). Maternal H3K27me3 controls DNA methylation-independent imprinting. Nature *547*, 419–424.

Inoue, A., Jiang, L., Lu, F., and Zhang, Y. (2017b). Genomic imprinting of *Xist* by maternal H3K27me3. Genes Dev. *31*, 1927–1932.

Itoh, M., Yoshida, Y., Nishida, K., Narimatsu, M., Hibi, M., and Hirano, T. (2000). Role of Gab1 in heart, placenta, and skin development and growth factor- and cytokine-induced extracellular signal-regulated kinase mitogen-activated protein kinase activation. Mol. Cell. Biol. *20*, 3695–3704.

Kamimura, S., Hatanaka, Y., Hirasawa, R., Matsumoto, K., Oikawa, M., Lee, J., Matoba, S., Mizutani, E., Ogonuki, N., Inoue, K., et al. (2014). Establishment of paternal genomic imprinting in mouse prospermatogonia analyzed by nuclear transfer. Biol. Reprod. *91*, 120.

Kim, D., Langmead, B., and Salzberg, S.L. (2015). HISAT: a fast spliced aligner with low memory requirements. Nat. Methods *12*, 357–360.

Kishigami, S., Mizutani, E., Ohta, H., Hikichi, T., Thuan, N.V., Wakayama, S., Bui, H.T., and Wakayama, T. (2006). Significant improvement of mouse cloning technique by treatment with trichostatin A after somatic nuclear transfer. Biochem. Biophys. Res. Commun. *340*, 183–189.

Lee, J., Inoue, K., Ono, R., Ogonuki, N., Kohda, T., Kaneko-Ishino, T., Ogura, A., and Ishino, F. (2002). Erasing genomic imprinting memory in mouse clone embryos produced from day 11.5 primordial germ cells. Development *129*, 1807–1817.

Leighton, P.A., Ingram, R.S., Eggenschwiler, J., Efstratiadis, A., and Tilghman, S.M. (1995). Disruption of imprinting caused by deletion of the H19 gene region in mice. Nature *375*, 34–39.

Li, Z., Wan, H., Feng, G., Wang, L., He, Z., Wang, Y., Wang, X.J., Li, W., Zhou, Q., and Hu, B. (2016). Birth of fertile bimaternal offspring following intracytoplasmic injection of parthenogenetic haploid embryonic stem cells. Cell Res. *26*, 135–138.

Li, Z.K., Wang, L.Y., Wang, L.B., Feng, G.H., Yuan, X.W., Liu, C., Xu, K., Li, Y.H., Wan, H.F., Zhang, Y., et al. (2018). Generation of Bimaternal and Bipaternal Mice from Hypomethylated Haploid ESCs with Imprinting Region Deletions. Cell Stem Cell *23*, 665–676.e4.

Lin, S.P., Youngson, N., Takada, S., Seitz, H., Reik, W., Paulsen, M., Cavaille, J., and Ferguson-Smith, A.C.F. (2003). Asymmetric regulation of imprinting on the maternal and paternal chromosomes at the Dlk1-Gtl2 imprinted cluster on mouse chromosome 12. Nat. Genet. *35*, 97–102.

Liu, Z., Cai, Y., Wang, Y., Nie, Y., Zhang, C., Xu, Y., Zhang, X., Lu, Y., Wang, Z., Poo, M., and Sun, Q. (2018). Cloning of Macaque Monkeys by Somatic Cell Nuclear Transfer. Cell *172*, 881–887.e7.

Lu, F., and Zhang, Y. (2015). Cell totipotency: molecular features, induction, and maintenance. Natl. Sci. Rev. *2*, 217–225.

Matoba, S., and Zhang, Y. (2018). Somatic Cell Nuclear Transfer Reprogramming: Mechanisms and Applications. Cell Stem Cell *23*, 471–485.

Matoba, S., Inoue, K., Kohda, T., Sugimoto, M., Mizutani, E., Ogonuki, N., Nakamura, T., Abe, K., Nakano, T., Ishino, F., and Ogura, A. (2011). RNAi-mediated knockdown of Xist can rescue the impaired postimplantation development of cloned mouse embryos. Proc. Natl. Acad. Sci. USA *108*, 20621–20626.

Matoba, S., Liu, Y., Lu, F., Iwabuchi, K.A., Shen, L., Inoue, A., and Zhang, Y. (2014). Embryonic development following somatic cell nuclear transfer impeded by persisting histone methylation. Cell *159*, 884–895.

Matoba, S., Wang, H., Jiang, L., Lu, F., Iwabuchi, K.A., Wu, X., Inoue, K., Yang, L., Press, W., Lee, J.T., et al. (2018). Loss of H3K27me3 Imprinting in Somatic Cell Nuclear Transfer Embryos Disrupts Post-Implantation Development. Cell Stem Cell *23*, 343–354.e5.

Miri, K., Latham, K., Panning, B., Zhong, Z., Andersen, A., and Varmuza, S. (2013). The imprinted polycomb group gene Sfmbt2 is required for trophoblast maintenance and placenta development. Development *140*, 4480–4489.

Nagy, A., Gócza, E., Diaz, E.M., Prideaux, V.R., Iványi, E., Markkula, M., and Rossant, J. (1990). Embryonic stem cells alone are able to support fetal development in the mouse. Development *110*, 815–821.

Ogura, A., Inoue, K., Ogonuki, N., Noguchi, A., Takano, K., Nagano, R., Suzuki, O., Lee, J., Ishino, F., and Matsuda, J. (2000). Production of male cloned mice from fresh, cultured, and cryopreserved immature Sertoli cells. Biol. Reprod. *62*, 1579–1584.

Ogura, A., Inoue, K., and Wakayama, T. (2013). Recent advancements in cloning by somatic cell nuclear transfer. Philos. Trans. R Soc. Lond. B Biol. Sci. *368*, 20110329.

Okae, H., Matoba, S., Nagashima, T., Mizutani, E., Inoue, K., Ogonuki, N., Chiba, H., Funayama, R., Tanaka, S., Yaegashi, N., et al. (2014). RNA sequencing-based identification of aberrant imprinting in cloned mice. Hum. Mol. Genet. *23*, 992–1001.

Okamoto, I., Patrat, C., Thepot, D., Peynot, N., Fauque, P., Daniel, N., Diabangouaya, P., Wolf, J.P., Renard, J.P., Duranthon, V., et al. (2011). Eutherian mammals use diverse strategies to initiate X-chromosome inactivation during development. Nature *472*, 370–374.

Onishi, A., Iwamoto, M., Akita, T., Mikawa, S., Takeda, K., Awata, T., Hanada, H., and Perry, A.C.F. (2000). Pig cloning by microinjection of fetal fibroblast nuclei. Science *289*, 1188–1190.

Ono, Y., Shimozawa, N., Ito, M., and Kono, T. (2001). Cloned mice from fetal fibroblast cells arrested at metaphase by a serial nuclear transfer. Biol. Reprod. *64*, 44–50.

Paquet, D., Kwart, D., Chen, A., Sproul, A., Jacob, S., Teo, S., Olsen, K.M., Gregg, A., Noggle, S., and Tessier-Lavigne, M. (2016). Efficient introduction of specific homozygous and heterozygous mutations using CRISPR/Cas9. Nature *533*, 125–129.

Rideout, W.M., 3rd, Eggan, K., and Jaenisch, R. (2001). Nuclear cloning and epigenetic reprogramming of the genome. Science *293*, 1093–1098.

Sado, T., and Sakaguchi, T. (2013). Species-specific differences in X chromosome inactivation in mammals. Reproduction *146*, R131–R139.

Schnieke, A.E., Kind, A.J., Ritchie, W.A., Mycock, K., Scott, A.R., Ritchie, M., Wilmut, I., Colman, A., and Campbell, K.H.S. (1997). Human factor IX transgenic sheep produced by transfer of nuclei from transfected fetal fibroblasts. Science *278*, 2130–2133.

Smith, L.C., Suzuki, J., Jr., Goff, A.K., Filion, F., Therrien, J., Murphy, B.D., Kohan-Ghadr, H.R., Lefebvre, R., Brisville, A.C., Buczinski, S., et al. (2012). Developmental and epigenetic anomalies in cloned cattle. Reprod. Domest. Anim. *47* (*Suppl 4*), 107–114.

Tamashiro, K.L.K., Wakayama, T., Akutsu, H., Yamazaki, Y., Lachey, J.L., Wortman, M.D., Seeley, R.J., D'Alessio, D.A., Woods, S.C., Yanagimachi, R., and Sakai, R.R. (2002). Cloned mice have an obese phenotype not transmitted to their offspring. Nat. Med. *8*, 262–267.

Tanaka, S., Oda, M., Toyoshima, Y., Wakayama, T., Tanaka, M., Yoshida, N., Hattori, N., Ohgane, J., Yanagimachi, R., and Shiota, K. (2001). Placentomegaly in cloned mouse concepti caused by expansion of the spongiotrophoblast layer. Biol. Reprod. *65*, 1813–1821.

Trapnell, C., Williams, B.A., Pertea, G., Mortazavi, A., Kwan, G., van Baren, M.J., Salzberg, S.L., Wold, B.J., and Pachter, L. (2010). Transcript assembly and quantification by RNA-Seq reveals unannotated transcripts and isoform switching during cell differentiation. Nat. Biotechnol. *28*, 511–515.

Tucci, V., Isles, A.R., Kelsey, G., and Ferguson-Smith, A.C.; Erice Imprinting Group (2019). Genomic Imprinting and Physiological Processes in Mammals. Cell *176*, 952–965.

Wakayama, T., and Yanagimachi, R. (1999). Cloning of male mice from adult tail-tip cells. Nat. Genet. *22*, 127–128.

Wakayama, T., and Yanagimachi, R. (2001). Mouse cloning with nucleus donor cells of different age and type. Mol. Reprod. Dev. *58*, 376–383.

Wakisaka-Saito, N., Kohda, T., Inoue, K., Ogonuki, N., Miki, H., Hikichi, T., Mizutani, E., Wakayama, T., Kaneko-Ishino, T., Ogura, A., and Ishino, F. (2006). Chorioallantoic placenta defects in cloned mice. Biochem. Biophys. Res. Commun. *349*, 106–114.

Xia, W., Xu, J., Yu, G., Yao, G., Xu, K., Ma, X., Zhang, N., Liu, B., Li, T., Lin, Z., et al. (2019). Resetting histone modifications during human parental-to-zygotic transition. Science *365*, 353–360.

Yang, X., Smith, S.L., Tian, X.C., Lewin, H.A., Renard, J.P., and Wakayama, T. (2007). Nuclear reprogramming of cloned embryos and its implications for therapeutic cloning. Nat. Genet. *39*, 295–302.

Zhang, W., Chen, Z., Yin, Q., Zhang, D., Racowsky, C., and Zhang, Y. (2019). Maternal-biased H3K27me3 correlates with paternal-specific gene expression in the human morula. Genes Dev. *33*, 382–387.

Zhao, X.Y., Li, W., Lv, Z., Liu, L., Tong, M., Hai, T., Hao, J., Guo, C.L., Ma, Q.W., Wang, L., et al. (2009). iPS cells produce viable mice through tetraploid complementation. Nature *461*, 86–90.

Zhou, Q., Renard, J.P., Le Friec, G., Brochard, V., Beaujean, N., Cherifi, Y., Fraichard, A., and Cozzi, J. (2003). Generation of fertile cloned rats by regulating oocyte activation. Science *302*, 1179.

Zou, H., Yu, D., Du, X., Wang, J., Chen, L., Wang, Y., Xu, H., Zhao, Y., Zhao, S., Pang, Y., et al. (2019). No imprinted XIST expression in pigs: biallelic XIST expression in early embryos and random X inactivation in placentas. Cell. Mol. Life Sci. *76*, 4525–4538.

STAR★METHODS

KEY RESOURCES TABLE

REAGENT or RESOURCE	SOURCE	IDENTIFIER
Antibodies		
GAB1	Cell Signaling Technology	Cat# 3232; RRID: AB_2304999
JADE1	Abcam	Cat# ab225696; RRID:AB_2832999
SFMBT2	Proteintech	Cat# 25256-1-AP; RRID:AB_2833000
CDX2	Biogenex	Cat# AM392; RRID AB_2650531
LAMINα1	Sigma	Cat# L9393; RRID: AB_477163
SMOC1	Abcam	Cat# ab200219; RRID:AB_2833001.
TUBULIN	Sigma	Cat# T6199; RRID: AB_477583
OCT3/4	Santa Cruz	Cat# sc-9081; RRID: AB_2167703
Chemicals, Peptides, and Recombinant Proteins		
PMSG	ProSpec	Cat# HOR-272
hCG	ProSpec	Cat# HOR-250
M2	Sigma	Cat# M7167
M16	Sigma	Cat# M7292
KSOM	Millipore	Cat# MR-020P-D
Vectashield with 4',6-diamidino-2-phenylindole (DAPI)	Beyotime	Cat# C1002
Pronase	Sigma	Cat# P8811
Cytochalasin B	Abcam	Cat# Ab143482
CHIR99021	Stemgent	Cat# 04-0004
PD0325901	Stemgent	Cat# 04-0006
LIF	Millipore	Cat# ESG1107
Hoechst 33342	Invitrogen	Cat# H3570
G418	GIBCO	Cat# 11811031
Puromycin	GIBCO	Cat# A1113803
GenomOne CF	Ishihara Sangyo	Cat# CF001
Critical Commercial Assays		
PureLinkTM RNA Mini Kit	Life	Cat# 12183018A
HiScript III 1st Strand cDNA Synthesis Kit	Vazyme	Cat# R312
pClone007 Blunt Vector Kit	TsingKe	Cat# TSV-007B
PCR DIG Probe Synthesis Kit	Roche	Cat# 11636090910
Deposited Data		
RNA-seq data	This paper	CRA002383 (https://bigd.big.ac.cn/gsa/)
Experimental Models: Cell Lines		
Mouse: haploid embryonic stem cells	This paper	N/A
Mouse: embryonic fibroblast cells	This paper	N/A
Mouse: tail fibroblast cells	This paper	N/A
Experimental Models: Organisms/Strains		
Mouse: B6D2F1 (C57BL/6XDBA/2)	Beijing Vital River	Cat# 302; RRID: MGI:5649818
Mouse: CD-1	Beijing Vital River	Cat# 201; RRID: MGI:5659424
PWK/Phj	The Jackson Laboratory	Cat# 003715; RRID: IMSR_JAX:003715
C57BL/6-Tg(CAG-EGFP)1Osb/J	The Jackson Laboratory	Cat# 003291; RRID: IMSR_JAX:003291
Oligonucleotides		
PCR Primers and sgRNAs	Table S4	BGI

(*Continued on next page*)

Continued

REAGENT or RESOURCE	SOURCE	IDENTIFIER
Software and Algorithms		
IMARIS	Bitplane	https://imaris.oxinst.com
GraphPad Prism 6	GraphPad Prism	https://www.graphpad.com/scientific-software/prism/
ImageScope (v12.0.1.5027)	Leica	https://www.leicabiosystems.com/digital-pathology/manage/aperio-imagescope/
HISAT2 (version 2.1.0)	HISAT	http://daehwankimlab.github.io/hisat2/
Cufflinks (version 2.2.1)	Cufflinks	http://cole-trapnell-lab.github.io/cufflinks/

RESOURCE AVAILABILITY

Lead Contact

Further information and requests for resources and reagents should be directed to and will be fulfilled by the Lead Contact, Qi Zhou (zhouqi@ioz.ac.cn).

Materials Availability

This study did not generate new unique reagents.

Data and Code Availability

The accession number for sequencing data reported in this paper is GSA: CRA002383 (https://bigd.big.ac.cn/gsa/). The list of software for data analysis and processing can be found in the Key Resources Table.

EXPERIMENTAL MODEL AND SUBJECT DETAILS

Animal care and use

All mouse experiments were performed in accordance with the Guidelines for the Use of Animals in Research issued by the Institute of Zoology, Chinese Academy of Sciences. All mice were housed in the animal facilities of the Chinese Academy of Sciences. B6D2F1 (C57BL/6 × DBA/2), C57BL/6, and CD-1 background mice were purchased from Beijing Vital River Laboratory. PWK/PhJ (Stock No. 003715) mice and C57BL/6-Tg(CAG-EGFP)1Osb/J (Stock No. 003291) were purchased from Jackson Laboratory. Male C57BL/6 mice were used to mate with the Δ4-NT-mice to derive offspring carrying separated noncanonical imprinting gene deletions. Female C57BL/6-Tg(CAG-EGFP)1Osb/J × PWK/PhJ mice were used to provide cumulus cells for nuclear transfer. Female B6D2F1 mice (C57BL/6 × DBA/2) were used to provide somatic donor cells and oocytes, and CD-1 background mice were used to provide fertilized embryos and as pseudopregnant surrogates.

METHOD DETAILS

Oocyte collection

Eight-week-old female mice were super-ovulated by consecutive injection of pregnant mare serum gonadotropin (PMSG) and human chorionic gonadotropin (hCG) (Ningbo Second Hormone Factory). Oocytes were collected from the oviduct 13–15 h after hCG injection. Derived oocytes were washed with HEPES-CZB and cultured in M16 medium (Sigma) as previously described (Kishigami et al., 2006). Cumulus cells were removed using hyaluronidase (ICN Pharmaceuticals). Before micromanipulation, the oocytes were cultured in CZB medium supplemented with 3 mg/mL BSA at 37°C, 5% CO_2.

CRISPR-Cas9 mediated gene deletions

We constructed one pair of sgRNAs for each deletion (Table S4). The targeted regions of H3K27me3-imprinting genes were the common exon of all alternative transcripts, and the targeted region of Xist included exons 1–6. Plasmid-encoding sgRNAs and Cas9 were transfected into 10^6 haESCs with neon (Invitrogen). Two days later, transfected haESCs were sorted by FACS based on GFP fluorescence and seeded on feeder cells at a low density, and 7 days after that, single colonies were picked for expansion and PCR detection for deletions (Table S4). Different from the way we derived the MEFs with quadruple noncanonical imprinting gene deletions, we generated the ΔXist/Δ4-MEFs^{3KO} by directly transfecting the Δ4-MEFs^{3KO} with Cas9 and Xist-deleting sgRNA expressing plasmids. The nuclei of transfected Δ4-MEFs^{3KO} were cloned by transferring into enucleated oocytes, and the reconstructed embryos were transferred into pseudopregnant recipients. Viable E13.5 embryos were recovered by cesarean section to derive MEFs. Embryos with objective monoallelic Xist deletion were screened by PCR and confirmed by Sanger sequencing. The Xist$^{\Delta/Y}$ mouse was derived by injecting Cas9 and Xist-deleting sgRNA expressing plasmids into one-cell-embryo of C57BL6 mice. Genotypes of

derived mice were confirmed by PCR and Sanger sequencing. Female mice conceiving Xist deletion were mated with C57BL6 male mice to derive the $Xist^{\Delta/Y}$ mouse. Genotype of the $Xist^{\Delta/Y}$ mouse was confirmed by Southern blot.

Intracytoplasmic injection of Δ4-haESCs^{3KO}

The Δ4-haESCs^{3KO} injection procedure was modified from a published protocol (Li et al., 2018). In brief, mature MII oocytes were collected from the oviduct of super-ovulated 8-week-old female mice (B6D2F1). FACS-sorted G0- or G1-phase Δ4-haESCs^{3KO} cells were chosen as donors. Before the microinjection of Δ4-haESCs^{3KO}, oocytes were pre-activated using 10 mM $SrCl_2$ (Sigma) in calcium-free CZB medium for 30 min. Sorted Δ4-haESCs^{3KO} were injected into oocytes separately to construct diploid embryos, which were then activated using 10 mM $SrCl_2$ in calcium-free CZB medium at 37°C and 5% CO_2 for another 5 h. Completely activated embryos were washed and cultured in M16 medium (Sigma) at 37°C under 5% CO_2 (Li et al., 2016). On the next day, reconstructed embryos at two-cell stage were directly transferred to pseudopregnant CD-1 recipients or cultured in KSOM medium (Millipore) to develop into blastocysts.

Blastocyst analysis by immunostaining

All blastocysts were treated by 5mg/mL pronase (Sigma) at 37°C (5% CO2, air) for 5–10 min to remove zona pellucida, and then washed in M16 (Sigma) and fixed with 4% paraformaldehyde (PFA) at room temperature for 30 min. After that, all fixed blastocysts were washed by PBS and permeabilized in 1% Triton X-100 in PBS at room temperature for 30 min, and blocked in 0.1% Tween-20, 0.01% Triton X-100 and 1% BSA in PBS at room temperature for 1 hour. Blocked blastocysts were incubated with primary antibodies (CDX2 and GAB1/JADE1/SMOC1) at 4°C overnight. Secondary antibodies were incubated at room temperature for 1 hour. Used secondary antibodies included Alexa 488 donkey anti-mouse (Invitrogen) and Cyanine3 goat anti-rabbit (Invitrogen). DNA contents were stained by DAPI (4′,6-diamidino-2-phenylindole, 5 μg/ml, Beyotime) incubation at room temperature for 5 min. To compare the extra-embryonic protein levels of H3K27me3-dependent imprinting genes, the relative fluorescence strength of GAB1, JADE1, and SMOC1 in dozens to hundreds of trophectoderm (TE) cells from the IVF, WT-NT, and Δ4-NT blastocysts were analyzed. TE cells with positive CDX2 signals were chosen for analyzing. Specific values of GAB1/JADE1/SMOC1 protein/DAPI signal ratios in each chosen TE cell were recorded (Leica SP8) and analyzed (IMARIS 3D/4D Visualization & Analysis Software).

Tetraploid embryo complementation of ICM cells

To derive the ICM of Δ4-embryo^{3KO} for tetraploid complementation, the zona pellucida of the embryo was removed by treatment with Pronase solution (Sigma) at 37°C for 3 min. Then the zona-free blastocysts were incubated in DMEM (GIBCO) containing 10% FBS (GIBCO) supplemented with 20% anti-mouse whole serum (Sigma) at 37°C for 3 h. After that, the blastocysts were washed with DMEM/FBS (10%) medium and incubated in 100% mouse serum for 20 min. The TE cells were removed by gentle pipetting, and the isolated ICM cells were placed in HER/FBS medium (GIBCO) before tetraploid complementation.

The derivation of tetraploid blastocysts for complementation was carried out as previously described (Zhao et al., 2009). In brief, two-cell embryos were collected from oviducts of CD-1 females and electrofused to produce tetraploid embryos before being cultured in CZB media. Then, 10–15 ICM cells were injected into each blastocyst and transferred to CD-1 pseudopregnant recipients.

Preparation of somatic donor cells for nuclear transfer

Primary MEFs were derived from E13.5 Δ4-embryos^{3KO} rescued by tetraploid blastocysts, E13.5 B6D2F1 embryos, and E13.5 embryos produced by intracytoplasmic injection of haESCs^{3KO}. After the removal of the head and organs, minced tissue from the remaining embryo was dissociated in 2 mL 0.25% Trypsin (GIBCO) with 1 mM EDTA (Thermo Fisher Scientific) at 37°C for 10 min. Cell suspension was diluted with an equal amount of DMEM (Thermo Fisher Scientific) containing 10% FBS (Thermo Fisher Scientific) and penicillin/streptomycin (Thermo Fisher Scientific), and it was pipetted more than 20 times. The cell suspension was diluted with fresh medium and plated onto 100 mm dishes and cultured at 37°C for 2 days before being harvested and frozen (passage 0). MEFs were used at passage 1 for all experiments.

TTFs were collected from the tail tip tissue of 6-week-old Δ4-NT-mice^{3KO}, B6D2F1 mice, and mice produced by intracytoplasmic injection of haESCs^{3KO}. Cut tail tip tissue (2-3 mm long) were placed on the bottom of culture dishes precoated with fibronectin and left to dry at 25–27°C for 10 min. After that, DMEM containing 10% FBS was added gently to avoid the detaching of tissues from the dish bottom. The tissues were cultured at 37°C until fibroblast cells divided and became confluent on the bottom (passage 0). TTFs were used before passage 3 for all experiments. Single-deletion TTFs were derived as described above.

Cumulus cells were collected from 8-week-old females (B6/PWK) through superovulation by injecting 7.5 IU of PMSG and 7.5 IU of hCG. After 15–17 h, cumulus cells were detached from the oocytes using hyaluronidase 300 IU/mL (ICN Pharmaceuticals). Before micromanipulation, oocytes were cultured in CZB (Cold Spring Harbor Laboratory) medium supplemented with 3 mg/mL BSA, covered with paraffin oil, and incubated at 37° and 5% CO_2. Cumulus cell suspensions were washed twice with HEPES-CZB medium and stored at 4°C before use.

Somatic cell nuclear transfer and embryo culture

SCNT was performed using the "one-step method" initially reported by Zhou et al. (2003). For cumulus cell cloning, cell nuclei were injected into the enucleated oocytes using a Piezo-driven micromanipulator. For fibroblast cloning, cells were fused with enucleated oocytes using the envelope of inactivated Sendai virus (GenomOne). Reconstructed embryos were incubated in M16 for 1 h, before

being activated in calcium-free CZB containing 5 mg/mL cytochalasin B (Abcam) and 10 mM SrcI2 (Sigma) for 5–6 h, after which the embryos were transferred into M16 and cultured with 5% CO_2 at 37°C.

In some experiments, 5 nM trichostatin A (Sigma) was added into the culture medium since activation and lasted for 10 h. For the modified SCNT culture media (D-media), the reconstructed embryos were cultured in M16 for 18–22 h and transferred into KSOM and cultured for 3.5 days in 5% CO_2 at 37°C.

Embryo transfer

Two-cell stage SCNT embryos or complemented tetraploid blastocysts were transferred into the uterus of E0.5 or E2.5 pseudopregnant CD-1 surrogate mothers, respectively. The pregnant recipients were sacrificed at E13.5 or E19.5, and all full-term pups were gestated by CD-1 surrogate mothers.

Immunohistochemistry staining and histological analysis

Placentae of full-term pups were fixed in 4% paraformaldehyde, followed by paraffin embedding and sectioning. Serial sections (4 mm thick) were subjected to HE staining, which was performed following standard procedures. To perform immunohistochemistry, the slides were rinsed in PBS for 5 min, and then incubated with blocking buffer (PBS with 1% BSA, 0.1% Tween-20) at room temperature for 20 min, followed by incubation with added primary antibodies for 1 h. After that, slides were washed with 0.1% Tween-20 in PBS for three times, and incubated with secondary antibodies in blocking buffer for 1 h. Slides were mounted with DAPI-Vectashield solution (Vector Laboratories). Images were taken with a panoramic tissue cell analyzer (Leica Aperio VESA8). Placental physiological parameters, including the areas of the trophoblast, acellular discontinues, and blood vessels, were analyzed with ImageScope (v12.0.1.5027).

Placental RNA extraction and reverse transcription PCR

Full-term placentae were digested and sorted for GFP positive cells by FACS. The RNAs of GFP positive cells were extracted using PureLink^{TM} RNA Mini Kit (Life). The reverse transcription of RNA was performed using the HiScript III 1st Strand cDNA Synthesis Kit (Vazyme), after removing DNA using the gDNA wiper provided in the kit. PCR fragments covering SNPs between PWK and C57 were amplified with primers designed by PrimerPremier5 (Table S4). The pClone007 Blunt Vector Kit (TsingKe) was used to link the RT-PCR product. After transformation, single colonies were picked after 12 h culture in 37°C, and analyzed by Sanger sequencing.

RNA-Seq library preparation and data analysis

In order to obtain the fetal-derived cells, the placentae were cut up and digested with 0.25% trypsin for 10-15 minutes at 37°C (5% CO_2, air). The tissues were pipetted for several times during the process of digestion. After that, the GFP positive placental cells were sorted and collected by FACS and sent for RNA-Seq analysis (BerryGenomics). For the mice transcriptome analyses, brains of WT mice, Δ4-NT-mice^{3KO}, and offspring mice were collected for RNA-seq. Each sample was with two biological repeats, and the brains of two Sfmbt2$^{\Delta/+}$ offspring from the early litters were applied as the offspring samples. Total RNA was extracted from fetus by TRIzol reagent (Invitrogen), after which 1 μg of purified RNA was used for reverse transcription polymerase reaction each time (Invitrogen). For RNA-seq library construction, two rounds of PolyA+ tailed RNA purification were performed for each sample. Sequencing was performed on an Illumina HiSeq 4000 sequencer with 150 bp paired-end sequencing reaction. RNA-seq data analysis was performed with HISAT2 (version 2.1.0) and Cufflinks (version 2.2.1) using the UCSC mm10 annotation with default settings (Kim et al., 2015; Trapnell et al., 2010). Normalized expression level FPKM for each gene was used for the next analysis. Reads with unique genome location were used for differentially expressed gene analysis using Cuffdiff using default parameters. And two-fold changes and p value = 0.05 from Cuffdiff were used as the cutoff. Genes with no less than 1 FPKM in at least one samples were transformed by log2 and used to produce scatterplots by R. To exhibit the parental expression biases of imprinting genes, the allele-specific read numbers of detected canonical imprinting genes (total reads number > 10 in all samples) were counted for analysis (Table S1). All read counts were added by 1 before division.

Western blot

In order to obtain fresh placental cells developed from fetuses, we cut up the placentae and digested them with 0.25% trypsin for 10–15 minutes at 37°C (5% CO2, air), and pipetted the tissues several times during the process of digestion. Then the GFP positive placental cells were sorted and collected by FACS. Placenta cells or haESCs were lysed in Pierce IP Lysis Buffer (Pierce), supplemented with Protease Inhibitor Cocktail (Pierce) and sodium orthovanadate (Sigma) on ice for 30 min. After a 12,000 rpm centrifugation at 4°C for 10 min, supernatants were collected and mixed with 30 μL sample buffer (10 mL; 1.25 mL 0.5 M pH 6.8 Tris-HCl, 2.5 mL glycerin, 2 mL 10% SDS, 200 μL 0.5% bromophenol blue, 3.55 mL H2O, and 0.5 mL β-mercaptoethanol) and incubated in boiling water for 5 min. The samples were separated by SDS-PAGE using a 5% stacking gel (10 mL; 5.7 mL ddH_2O, 2.5 mL 1.5 M pH 6.8 Tris-HCl, 1.7 mL 30% acrylamide [acryl:bis acryl = 29:1], 100 μL 10% SDS, 50 μL 10% ammonium persulfate, and 10 μL TEMED) and a 10% separating gel (10 mL; 4.1 mL ddH_2O, 2.5 mL 1.5 M pH 8.8 Tris-HCl, 3.3 mL 30% acrylamide [acryl:bis acryl = 29:1], 100 μL 10% SDS, 50 μL 10% ammonium persulfate, and 5 μL TEMED) at 100 V for 1 h, and then electrophoretically transferred onto a nitrocellulose membrane at 200 mA at 4°C for 1 h. Membranes were blocked in TBST buffer (10 mM Tris, 150 mM NaCl, 0.1% Tween 20, pH 7.4) containing 3% BSA (Sigma) at RT for 1 h, and then incubated with primary antibody that

diluted in TBST containing 1% BSA at 4°C overnight. After being washed three times (10 min each time) in TBST, the membrane was incubated for 1 h at RT with the secondary antibody diluted in TBST. The signals were detected using ECL after being washed three times (10 min each time),

Southern blot

Genomic DNA was extracted from mouse tissues and digested with endonucleases (Takara) overnight at 37°C. Digested DNA fragments were separated by agarose gel (0.8%) and transferred to a positively charged nylon membrane (Roche) for hybridization. The digoxigenin-labeled probe for each deletion was amplified by PCR with synthesized primers (Table S4). Hybridization and detection were performed according to the manufacturer's instruction of PCR DIG Probe Synthesis Kit (Roche).

QUANTIFICATION AND STATISTICAL ANALYSIS

Statistical analyses were performed in R. Levels of significance were calculated using the two-tailed Student's t test. In all figures: *, p value < 0.05; **, p value < 0.01, ***, p value < 0.001; ****, p value < 0.0001. For statistical analysis, GraphPad Prism was used.